THE JOURNAL OF BIOLOGICAL CHEMISTRY VOL. 289, NO. 22, pp. 15350–15362, May 30, 2014
Published in the U.S.A.

Inhibition of Cellular Methyltransferases Promotes Endothelial Cell Activation by Suppressing Glutathione Peroxidase 1 Protein Expression*

Received for publication, January 11, 2014, and in revised form, April 3, 2014 Published, JBC Papers in Press, April 9, 2014, DOI 10.1074/jbc.M114.549782

Madalena Barroso[‡§], Cristina Florindo[§], Hermann Kalwa[‡], Zélia Silva[¶], Anton A. Turanov[‖], Bradley A. Carlson[**], Isabel Tavares de Almeida[§‡‡], Henk J. Blom[§§], Vadim N. Gladyshev[‖], Dolph L. Hatfield[**], Thomas Michel[‡], Rita Castro[§‡‡], Joseph Loscalzo[‡], and Diane E. Handy[‡1]

*From the [‡]Cardiovascular and [‖]Genetics Divisions, Department of Medicine, Brigham and Women's Hospital and Harvard Medical School, Boston, Massachusetts 02115, the [§]Research Institute for Medicines and Pharmaceutical Sciences (iMed.UL) and [‡‡]Department of Biochemistry and Human Biology, Faculty of Pharmacy, University of Lisbon, 1649-004 Lisbon, Portugal, the [¶]Chronic Diseases Research Center, Departamento de Imunologia, Faculdade de Ciências Médicas, Universidade Nova de Lisboa, 1099-085 Lisbon, Portugal, the **Molecular Biology of Selenium Section, Mouse Cancer Genetics Program, National Cancer Institute, National Institutes of Health, Bethesda, Maryland 20892, and the [§§]Department of General Pediatrics, Center for Pediatrics and Adolescent Medicine, University Hospital, 79106 Freiburg, Germany*

Background: Methylation of $tRNA^{Sec}$ facilitates the incorporation of selenocysteine at a UGA codon during translation.
Results: Accumulation of the homocysteine precursor *S*-adenosylhomocysteine decreases $tRNA^{Sec}$ methylation, reducing glutathione peroxidase 1 expression and increasing oxidative stress-induced inflammatory activation of endothelial cells.
Conclusion: Methylation modulates the expression of selenoproteins to regulate redox-dependent inflammatory pathways.
Significance: Hypomethylation stress promotes a proatherogenic endothelial cell phenotype.

S-Adenosylhomocysteine (SAH) is a negative regulator of most methyltransferases and the precursor for the cardiovascular risk factor homocysteine. We have previously identified a link between the homocysteine-induced suppression of the selenoprotein glutathione peroxidase 1 (GPx-1) and endothelial dysfunction. Here we demonstrate a specific mechanism by which hypomethylation, promoted by the accumulation of the homocysteine precursor SAH, suppresses GPx-1 expression and leads to inflammatory activation of endothelial cells. The expression of GPx-1 and a subset of other selenoproteins is dependent on the methylation of the $tRNA^{Sec}$ to the Um34 form. The formation of methylated $tRNA^{Sec}$ facilitates translational incorporation of selenocysteine at a UGA codon. Our findings demonstrate that SAH accumulation in endothelial cells suppresses the expression of GPx-1 to promote oxidative stress. Hypomethylation stress, caused by SAH accumulation, inhibits the formation of the methylated isoform of the $tRNA^{Sec}$ and reduces GPx-1 expression. In contrast, under these conditions, the expression and activity of thioredoxin reductase 1, another selenoprotein, is increased. Furthermore, SAH-induced oxidative stress creates a proinflammatory activation of endothelial cells characterized by up-regulation of adhesion molecules and an augmented capacity to bind leukocytes. Taken together, these data suggest that SAH accumulation in endothelial cells can induce $tRNA^{Sec}$ hypomethylation, which alters the expression of selenoproteins such as GPx-1 to contribute to a proatherogenic endothelial phenotype.

S-Adenosylhomocysteine (SAH)[2] is an intermediate of homocysteine (Hcy) metabolism, which, in excess, is a feedback inhibitor of most cellular methylation processes. Methyltransferases use *S*-adenosylmethionine (AdoMet) to methylate a wide range of substrates, such as DNA, RNA, proteins, and other biomolecules, and SAH is generated by every AdoMet-dependent methylation reaction (1, 2). During hyperhomocysteinemia, which is an independent risk factor for cardiovascular disease, the Hcy precursor SAH accumulates as well because the reaction catalyzed by SAH hydrolase (SAHH) thermodynamically favors SAH synthesis over its hydrolysis to Hcy. DNA hypomethylation has been correlated with increased levels of SAH in mice and humans with hyperhomocysteinemia (3, 4). More recently, we have shown that increased levels of SAH also lead to protein arginine hypomethylation in rodents (5, 6).

We have reported previously that Hcy can induce oxidative stress through glutathione peroxidase 1 (GPx-1) down-regulation by decreasing its translation. However, the underlying mechanism remains unknown (7). GPx-1 is a major antioxidant

* This work was supported, in whole or in part, by National Institutes of Health Grants HL067195, HL070819, HL048743, HL107192, and HL108630 (to J. L.); HL46457 and HL48743 (to T. M.); and GM061603 (to V. N. G.). This work was also supported by an American Heart Association postdoctoral fellowship grant (to H. K.) and by Portuguese Fundação para a Ciência e a Tecnologia Grants PTDC/SAU-ORG/112683/2009 (to R. C.) and SFRH/BD/73021/2010 (M. B.).

[1] To whom correspondence should be addressed: Cardiovascular Div., Dept. of Medicine, Brigham and Women's Hospital and Harvard Medical School, 77 Ave. Louis Pasteur, Boston, MA, 02115. Tel.: 617-525-4845; Fax: 617-525-4830; E-mail: dhandy@rics.bwh.harvard.edu.

[2] The abbreviations used are: SAH, *S*-adenosylhomocysteine; Hcy, homocysteine; AdoMet, *S*-adenosylmethionine; SAHH, *S*-adenosylhomocysteine hydrolase; GPx, glutathione peroxidase, ROS, reactive oxygen species; ICAM-1, intercellular adhesion molecule 1; VCAM-1, vascular cell adhesion molecule 1; Sec, selenocysteine; mcm^5U, 5-methoxycarbonylmethyluridine; mcm^5Um, 5-methoxycarbonylmethyl-2′-*O*-methyluridine; TrxR, thioredoxin reductase; HUVEC, human umbilical vein endothelial cell; ADA, adenosine-2′,3′-dialdehyde.

protein that uses GSH as a cofactor to reduce hydrogen peroxide (H_2O_2) to water and other hydroperoxides to their corresponding alcohols (8). Antioxidant agents such as GPx-1 are crucial for maintaining endothelial homeostasis. In fact, antioxidant deficiency may lead to intracellular accumulation of reactive oxygen species (ROS), creating oxidative stress (8, 9). Oxidative stress is a major contributor to atherosclerosis and vascular dysfunction. An increase in ROS leads to LDL oxidation, decreases NO bioavailability, and induces the activation of transcription factors such as NFκB to promote the expression of adhesion molecules such as intercellular adhesion molecule 1 (ICAM-1) and vascular cell adhesion molecule 1 (VCAM-1) (10–12). The binding and transmigration of leukocytes from the lumen of vessels into the vessel wall is mediated by the presence of these adhesion molecules at the endothelial cell surface (10, 13). Work by us and others has shown that GPx-1 deficiency can induce the expression of these key adhesion molecules by regulating ROS flux, thus promoting atherogenesis (14–17). Furthermore, decreased activity of GPx-1 has been shown to be independently associated with an increased risk of cardiovascular events in human subjects (17).

GPx-1 and its several paralogs (GPx-2, GPx-3, GPx-4, and GPx-6) are part of the human selenoproteome, which comprises proteins that carry selenium incorporated in their polypeptide chain in the form of the amino acid selenocysteine (Sec) (18). Selenoprotein expression relies on the ability of a Sec-carrying tRNA ($tRNA^{[Ser]Sec}$) to recognize UGA not as a stop codon but as the site of incorporation of Sec during translation. For this, additional cofactors are necessary (19). The selenoprotein-encoding transcripts contain a stem-loop structure (Sec insertion sequence) within their 3′ UTR which, together with translational cofactors, contribute to Sec incorporation (18, 19). Sec is synthesized on $tRNA^{[Ser]Sec}$, which is first aminoacylated with Ser and then enzymatically converted to Sec (20). The mammalian $tRNA^{[Ser]Sec}$ population consists of two major isoforms that differ by a single methyl group on the ribosyl moiety at position 34, 2′-*O*-methylribose (21). The highly modified base at position 34 is 5-methoxycarbonylmethyluridine (mcm^5U), and, thus, the two isoforms are designated mcm^5U and 5-methoxycarbonylmethyl-2′-*O*-methyluridine (mcm^5Um) (21). Loss of the isopentenyladenosine (iA6) at position 37 (*e.g.* by site substitution of adenosine-37 with guanosine) prevents 2′-*O*-methylribose (Um34) formation at position 34 (22). The adenosine-37 to guanosine-37 mutation or selenium deficiency conditions reduce Um34 formation and decrease the expression of a subset of selenoproteins, designated stress-related selenoproteins, such as GPx-1 and selenoprotein W. On the other hand, these changes have less effect on the expression of another subset of selenoproteins, designated housekeeping selenoproteins, such as the thioredoxin reductases TrxR1 and TrxR2 (21, 23).

In this study, we analyzed the link between SAH-induced hypomethylation and the expression of selenoproteins. We determined that SAH accumulation suppresses GPx-1 expression, in part, by altering the methylation of $tRNA^{[Ser]Sec}$. Additionally, hypomethylation of the $tRNA^{[Ser]Sec}$ altered the expression of other selenoproteins, as shown by [^{75}Se]-incorporation. Furthermore, the SAH-induced hypomethylation environment caused an increase in ROS levels and a subsequent up-regulation of adhesion molecules. These findings illustrate the functional consequences of hypomethylation on selenoprotein synthesis and cellular homeostasis and their clear implications for vascular pathology.

EXPERIMENTAL PROCEDURES

Cell Culture, Treatments, and siRNA Transfection—Human umbilical vein endothelial cells (HUVECs) were cultured in EBM-2 medium (Lonza) supplemented with EGM-2 additives (Lonza) without antibiotics at 37 °C in 5% CO_2. These culture conditions included 2% FBS, which added 7.5 nM selenium to the basal level of 30 nM selenium (in the form of selenious acid) in the basal medium. Selenium was added in the form of sodium selenite in some experiments, as noted in the figure legends. Experiments were performed between passages five and eight with cells 70–80% confluent. Cells were treated with 5–20 μM adenosine-2′,3′-dialdehyde (ADA) (Sigma) for 12–48 h. 8 mM *N*-acetylcysteine was used as an antioxidant in some experiments, as designated in the figure legends.

Transfections with siRNA were performed using Lipofectamine 2000 (Invitrogen). In each transfection, a final concentration of 60 nM siRNA (Invitrogen) to SAHH mRNA (5′-ACGCCGUGGAGAAGGUGAACAUCAA-3′) or GPx-1 mRNA (5′-GGUUCGAGCCCAACUUCAUGCUCUU-3′) was used. All transfections were performed in parallel with scrambled control siRNAs (5′-UUGGGAUUGUCCACUCUUCACCCGU-3′ for the SAHH control or (5′-GGUAGCGCCAAUCCUUACGUCUCUU-3′ for the GPx-1 control).

AdoMet/SAH Analysis and SAHH Activity—To measure SAH and AdoMet intracellular metabolites, cell lysates were promptly deproteinized with an equal volume of 10% perchloric acid and then quantified using tandem mass spectrometry, as described previously (24).

SAHH activity was measured in the hydrolytic direction using an assay on the basis of the reduction of 3-(4,5-dimethylthiazol-2-yl)-2,5-diphenyltetrazolium bromide to formazan according to published methods (25, 26). The assay was performed on cell lysates, comparing equivalent amounts of protein for each condition. Lysates were preincubated with 3-(4,5-dimethylthiazol-2-yl)-2,5-diphenyltetrazolium bromide for 5 min prior to adding SAH to monitor the SAHH-specific reduction of 3-(4,5-dimethylthiazol-2-yl)-2,5-diphenyltetrazolium bromide.

Real-time PCR—Total RNA was isolated using an RNeasy mini kit (Qiagen), and 0.5 μg of each sample was reverse-transcribed using an Advantage RT-for-PCR kit (Clontech). Relative mRNA quantification was performed by TaqMan assays using the PRISM 7900 HT sequence detector (Applied Biosystems). The ΔΔCt method of relative quantification was used to compare gene expression, using β-actin as an endogenous control. Real-time PCR reactions used TaqMan Universal PCR Master Mix (Invitrogen) and the following specific gene expression primers: 4352935E, β-actin; Hs00829989_gH, GPx-1; Hs00164932_m1, ICAM-1; Hs04183463_g1, SAHH; and Hs00365485_m1, VCAM-1 (Invitrogen).

Western Blotting—Antibodies to β-actin (Sigma-Aldrich), GPx-1 (Abcam), SAHH (R&D Systems), ICAM-1, VCAM-1 (Santa Cruz Biotechnology), or the antibodies described previously for TrxR1 or TrxR2 (27) were used as primary antibodies

for Western blotting. After 2 h of incubation with a secondary antibody linked to HRP, membranes were visualized using an ECL detection system (Amersham Biosciences).

GPx Activity Assay—An indirect assay on the basis of absorbance changes after NADPH oxidation was used to measure GPx-1 activity (27).

TrxR Activity Assay—The assay measures the direct reduction of 5,5′-dithiobis(2-nitrobenzoic acid) by thioredoxin reductase. To account for nonspecific reduction of 5,5′-dithiobis(2-nitrobenzoic acid) by other cellular enzymes, the change in 5,5′-dithiobis(2-nitrobenzoic acid) reduction over time in the presence of the TxR inhibitor aurothioglucose is subtracted from the activity in the absence of inhibitor to determine TrxR-specific activity (28, 29).

GPx-1 Overexpression—GPx-1 was expressed in endothelial cells using an adenoviral vector (AdGPx-1), as described previously (30). HUVECs were incubated with adenovirus for 24 h prior to exposure to ADA or control medium. An adenovirus expressing β-galactosidase (Ad-βGal) was used as a control.

ROS Measurements—ROS were assessed by two independent methods. First, hydrogen peroxide (H_2O_2) released by endothelial cells was measured by Amplex Red assay (Molecular Probes) using methods described previously (14). Intracellular H_2O_2 was monitored using the highly specific biosensor HyPer2 expressed in lentivirus (31–33). HUVECs were infected with virus particles (10^6 pfu/ml) in the presence of Polybrene (4 mM). Upon treatment, live cells were monitored, in parallel with control samples, for 13 h using a microscope stage incubator (Tokai) and an Olympus IX81 inverted microscope with a disk scanning unit spinning disk confocal system and a Hamamatsu Orca-ER cooled charge-coupled device camera. Image acquisition was performed using a ×40 oil immersion objective lens (Olympus) every 5 min. The HyPer2 fluorescence ratio was calculated as described previously (32, 33). For imaging of fixed cells, lentivirus-infected HUVECs were treated for 24 h and then washed and fixed with 4% paraformaldehyde in PBS for 20 min. Fixed cells were mounted using DAPI-containing mounting medium or DAPI-free mounting medium (SouthernBiotech) and imaged. Methamorph imaging software (Universal Imaging) was used for analysis.

Flow Cytometry and Static Adhesion Assay—ICAM-1 surface expression was analyzed after cell staining with FITC-conjugated anti-ICAM-1 antibody (Santa Cruz Biotechnology). Briefly, cells were trypsinized, washed with PBS, incubated with antibody for 30 min, washed with PBS containing 0.1% NaN_3, and analyzed using GUAVA EasyCyte 5HT FACS and InCyte software (Millipore).

An adhesion assay using human leukocytes was performed under static conditions. Leukocytes (WBC) were isolated from blood samples of healthy individuals using an RBC lysis solution (Citogene). The ethics committee at the Faculty of Pharmacy, University of Lisbon approved the study, and written informed consent was obtained from all participants. After three washes with PBS, WBCs were resuspended at 6×10^6 cells/ml in PBS with Ca^{2+} and Mg^{2+} with 0.1% human serum and added to the confluent HUVEC monolayer. The cell mixture was incubated for 20 min at 37 °C and 5% CO_2, after which cells were washed thoroughly with PBS without Ca^{2+} and Mg^{2+}, trypsinized, and assessed for cell-specific markers by flow cytometry. An antibody mixture of phycoerythrin anti-human CD31 antibody (BioLegend) and peridinin-chlorophyll-protein complex anti-human CD45 antibody (BioLegend) was used to distinguish endothelial and leukocyte cell populations, respectively.

[^{75}Se] Labeling—HUVECs were labeled with 10 μCi/ml of [^{75}Se]-selenious acid (1000 Ci/mmol, Research Reactor Facility, University of Missouri, Columbia, MO) for 24 h in cell culture medium supplemented with or without ADA (20 μM). Cells were then washed and lysed, and protein extracts were separated on 10% BisTris gels (NuPage, Novex, Invitrogen). Proteins were then transferred to a PVDF membrane (Invitrogen), exposed to Storage Phosphor Screen (GE) for 24 h, and analyzed with PhosphorImager (GE) (34). Finally, membranes were used for immunoblotting. Anti-β-actin antibody was used to confirm equal protein loading of the samples.

Sec-tRNA Analysis—1 g of HUVECs was used for total RNA isolation and aminoacylation with [^{3}H]serine and 19 unlabeled amino acids, as described previously (35, 36). The aminoacylated seryl-tRNA was fractionated on an RPC-5 column, first in the absence of Mg^{2+} and subsequently in the presence of Mg^{2+}. Using this sequential chromatography approach, it is possible to quantify the relative $tRNA^{[Ser]Sec}$ to the total $tRNA^{Ser}$ and separate the two major isoforms of $tRNA^{[Ser]Sec}$, mcm^5U and mcm^5Um (35, 36).

Statistics—Statistical analysis was performed on experiments repeated in three to five independent assays. The statistical significance of differences among means ($p < 0.05$) in experiments with more than two conditions was determined by analysis of variance, followed by pairwise post hoc comparisons with Student-Newman-Keuls test. Alternatively, Student's *t* test was used for comparison in experiments with only two groups.

RESULTS

SAH Accumulation in Endothelial Cells—SAH is a metabolite of methionine metabolism and an endogenous inhibitor of AdoMet-dependent methyltransferases. SAH accumulation was induced by two different approaches: direct inhibition of SAHH by ADA or targeted knockdown of SAHH using siRNA. ADA, an adenosine analog, is a strong inhibitor of SAHH activity that has been used previously by us and others (2, 37). Following HUVEC incubation with 20 μM ADA for 24 h, SAHH activity was reduced by 99.5 ± 0.8% ($p < 0.0001$) (Fig. 1). This treatment significantly decreased SAHH mRNA by 27.1 ± 2.9% ($p < 0.0001$) and 45.3 ± 2.9% ($p < 0.0001$) after 24 and 48 h, respectively, with no statistically significant change in protein expression over this time course. Using a specific siRNA against SAHH, enzymatic activity was suppressed by 66.5 ± 3.7% ($p < 0.0001$) 48 h after transfection, with corresponding decreases of 88.5 ± 6.5% ($p < 0.001$) and 48.3 ± 15.8% ($p < 0.01$) at the mRNA and protein levels, respectively. The AdoMet/SAH ratio, commonly used as an indicator of cell methylation status, was decreased by 6.1 ± 0.2-fold ($p < 0.001$) after 24-h incubation with 20 μM ADA and 1.3 ± 0.2-fold ($p < 0.005$) after 72 h of siSAHH transfection.

GPx-1 Activity under SAH Accumulation—Hcy levels and GPx-1 activity are strong biomarkers for cardiovascular risk, with clinical studies suggesting that those with the lowest

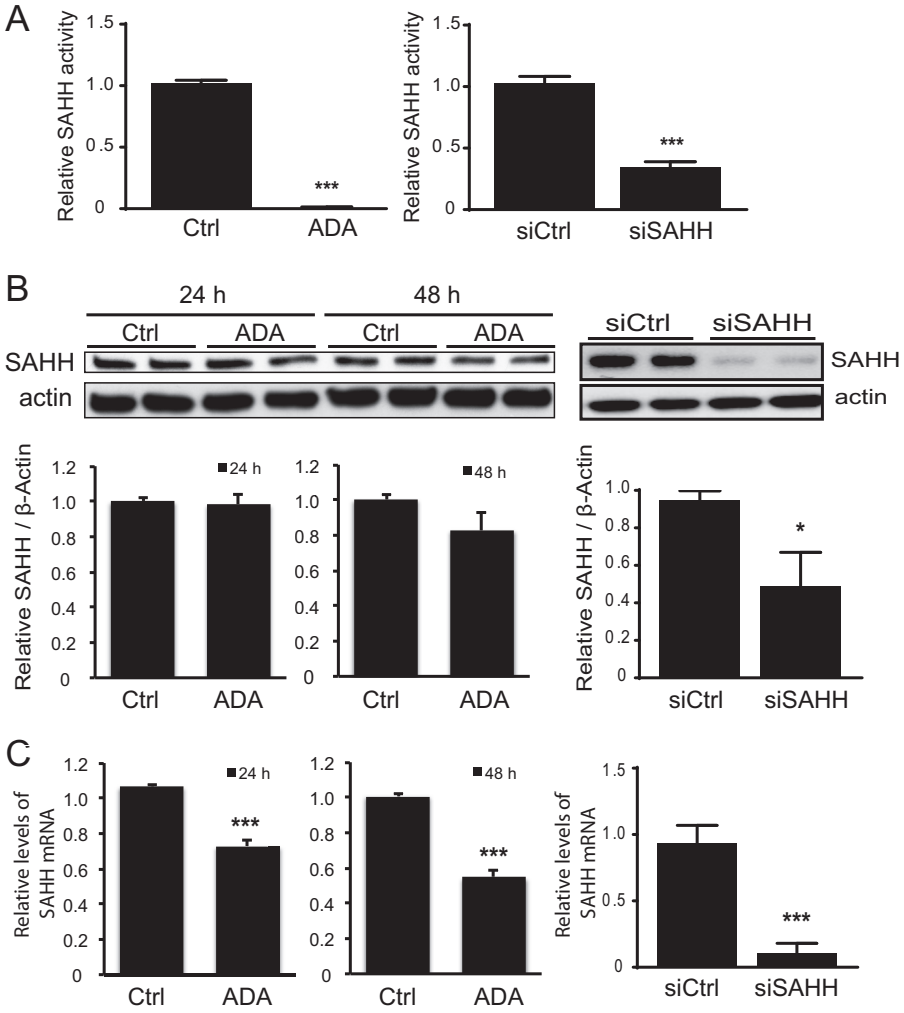

FIGURE 1. **Inhibition of cellular SAHH activity.** *A*, ADA or siSAHH was used to decrease SAHH activity. Means are significantly different by Student's *t* test. ***, $p < 0.0001$ *versus* control, $n = 3–4$. *Ctrl*, control. *B*, the effects of ADA or siSAHH on SAHH protein expression was examined by Western blotting. Summary densitometry measurements, corrected for actin intensity, are shown below the immunoblot analyses ($n = 3–4$). *, $p < 0.05$ *C*, the effects of ADA or siSAHH on SAHH mRNA were measured by quantitative RT-PCR, using actin as an endogenous control. **, $p < 0.001$; ***, $p < 0.0001$ *versus* control; $n = 3–4$.

GPx-1 activity are at the greatest risk (17, 38). Our previous studies have shown that excess Hcy suppresses GPx-1 expression by decreasing selenium-dependent translation. However, although these findings linked suppression of GPx-1 to conditions that favored the intracellular formation of SAH, a role for SAH in the translational regulation of GPx-1 remained unresolved (7, 39). To determine whether SAH modulates GPx-1 expression, we treated cells with ADA or siSAHH. Incubation of endothelial cells with increasing concentrations of the SAHH inhibitor, from 5 to 20 μM, resulted in a significant decrease of GPx-1 activity in a dose-dependent manner (Fig. 2*A*). ADA (20 μM) or the siRNA-mediated knockdown of SAHH significantly reduced GPx-1 protein expression by more than 27% (Fig. 2*B*). Under these conditions, however, GPx-1 mRNA levels were not altered significantly, which is consistent with the hypothesis that SAH-induced hypomethylation affects GPx-1 expression at a translational level (Fig. 2*C*).

Hypomethylation Induces Endothelial Oxidative Stress—The enzymatic actions of GPx-1 and other antioxidants diminish the damaging effects of ROS, like H_2O_2 (8). Thus, we next assessed whether the ADA-induced suppression of GPx-1 altered cellular H_2O_2 accumulation in endothelial cells. To do so, we measured cellular H_2O_2 levels by two different methods. First, we used the Amplex Red assay to quantitate extracellular H_2O_2 levels. After 24 h of exposure, we found an increase in H_2O_2 released to the medium with increasing ADA concentrations (Fig. 3*A*). Next, we used the biosensor Hyper2 to monitor intracellular H_2O_2 flux. Hyper2 is a biosensor that uses the regulatory domain of the *Escherichia coli* H_2O_2-sensing protein OxyR. The HyPer2 probe has a fluorescent protein (circularly permuted yellow fluorescence protein) inserted into the OxyR domain, which allows the detection of fluorescence changes when the domain undergoes oxidation by H_2O_2 (31). ADA induced a 2.5-fold increase in the production of intracellular H_2O_2 (Fig. 3*B*). These findings suggest that hypomethylation stress promotes an oxidative imbalance in endothelial cells, most likely because of the suppression of GPx-1.

Oxidative Stress Induced by SAH Accumulation Promotes Endothelial Cell Activation—Endothelial activation is a consequence of oxidative stress, characterized by an increase in the expression of inflammatory cytokines and adhesion molecules, which promote adhesion and transendothelial migration of leu-

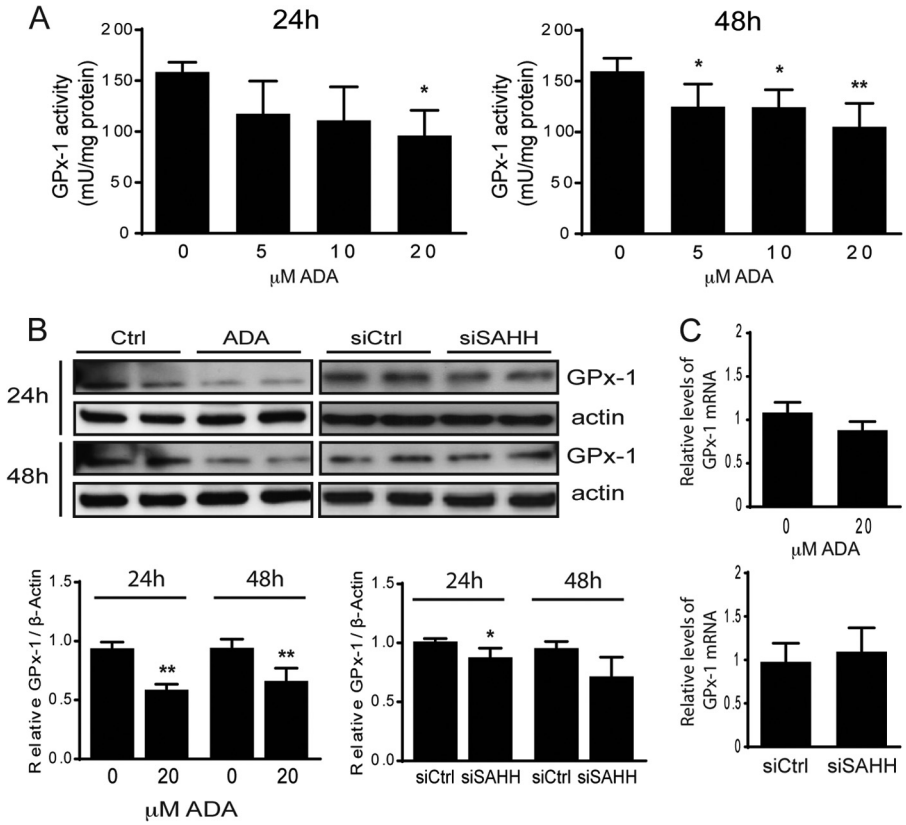

FIGURE 2. **Effect of SAH accumulation on GPx-1.** *A*, GPx-1 activity was measured by an indirect coupled enzymatic assay. Means were significantly different by analysis of variance, followed by post hoc pairwise comparisons ($n = 4–5$). *, $p < 0.05$; **, $p < 0.005$. *B*, the effect of SAHH inhibition on the expression of GPx-1 was examined by Western blotting. A representative blot (*top panel*) and summary densitometry measurements, corrected for actin intensity (*bottom panel*), are shown for 24 and 48 h in the presence and absence of ADA or siSAHH ($n = 3$). *, $p < 0.05$; **, $p < 0.005$. *C*, mRNA levels from the same experiments were measured by quantitative RT-PCR using actin as an endogenous control. No significant difference was found between treatment groups.

kocytes (40, 41). Thus, to determine whether SAH-induced oxidant stress augmented endothelial cell activation, we measured the expression of the adhesion molecules ICAM-1 and VCAM-1 following SAHH inhibition. Fig. 4 shows a positive correlation between a hypomethylation environment and adhesion molecule expression. Both ADA and siSAHH significantly induced ICAM-1 and VCAM-1 expression detectable at the protein (Figs. 4*A* and 5*A*) and transcript levels (Fig. 4*B*).

ICAM-1 and VCAM-1 expression have been associated with ROS levels, both under normal and under pathogenic conditions (10, 41, 42). Therefore, to causally link endothelial activation with SAH-induced oxidative stress, endothelial cells were coincubated with ADA and various antioxidants. Both ICAM-1 and VCAM-1 were induced by ~2-fold ($p < 0.05$) following ADA or siSAHH exposure (Figs. 4 and 5*A*). Treatment with the antioxidant *N*-acetyl-cysteine significantly attenuated the ADA-induced up-regulation of these adhesion molecules (Fig. 5*A*). A similar effect was found with the antioxidants butylated hydroxyanisole (100 μM) and allopurinol (150 μM) (data not shown). Similarly, overexpression of GPx-1 in endothelial cells minimized the effect of ADA exposure on adhesion molecule expression (Fig. 5*B*). The specific role of GPx-1 in regulating adhesion molecule expression was further assessed by performing a knockdown of this antioxidant protein. As shown in Fig. 5*B*, GPx-1 knockdown potentiated the ADA effect. ADA-induced ICAM-1 expression was increased 47.3% by the combination of siGPx-1 plus ADA compared with ADA alone ($p < 0.05$). VCAM-1 expression was also up-regulated by GPx-1 suppression, although the increase in expression was not significantly different between ADA and ADA treatment with GPx-1 knockdown. These findings are consistent with a role for excess ROS, caused by the suppression of GPx-1, in mediating the SAH-induced up-regulation of endothelial adhesion molecules.

Hypomethylation Increases the Endothelium Leukocyte-binding Capacity—We next sought to determine whether the ADA-induced up-regulation of ICAM-1 and VCAM-1 was sufficient to enhance leukocyte binding. We first confirmed that the induced up-regulation of ICAM-1 expression resulted in a corresponding increase in ICAM-1 at the cell surface, where it is capable of leukocyte binding. To do so, we used a fluorescently tagged antibody to ICAM-1 and evaluated changes in the mean fluorescence intensity by flow cytometry. Using this method, cell surface detection of ICAM-1 was significantly up-regulated by 1.6-fold at 48 h and by 2.1-fold at 72 h ($p < 0.05$) following ADA exposure (Fig. 6*A*). Next, to assess the leukocyte-binding capacity of these endothelial cells following hypomethylation stress, we performed an adhesion assay. In this assay, we coincubated endothelial cells (control cells or those previously exposed to ADA) with leukocytes for 20 min under static conditions. After several washes, cells were detached and stained with fluorescent anti-CD31 or anti-CD45 antibody to quantitate the number of endothelial cells ($CD31^+$) and leukocytes ($CD45^+$) by flow cytometry and to evaluate the number of leu-

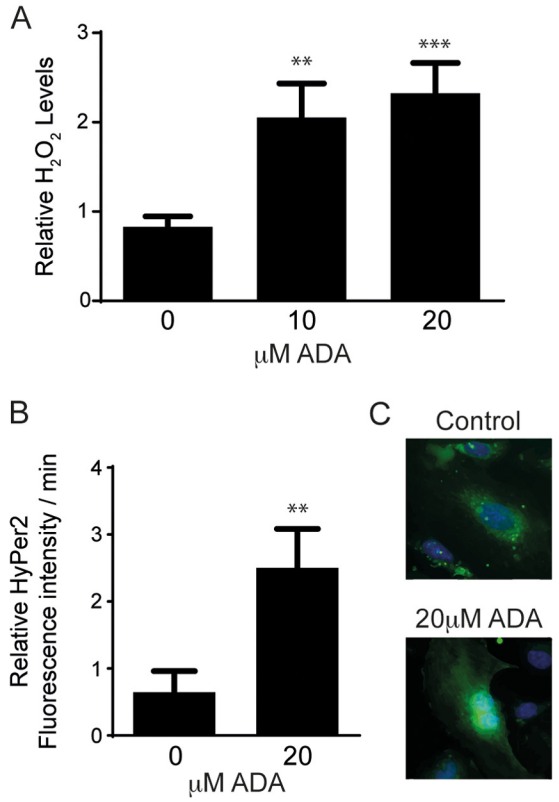

FIGURE 3. **H_2O_2 levels are increased by SAHH inhibition.** *A*, after 24 h of ADA exposure, H_2O_2 release from cells was measured by Amplex Red. The results represent means from three independent experiments that were analyzed by analysis of variance, followed by pairwise post hoc analysis. **, $p < 0.005$; ***, $p < 0.0005$ compared with control. *B*, intracellular H_2O_2 production was detected using the HyPer2 fluorescence ratio. The *graph* shows the means of three independent experiments, for which fluorescence ratios were measured for 3–5 cells/condition over 13 h. **, $p < 0.005$ compared with control. *C*, representative images of Hyper2-transfected cells 24 h following exposure to ADA-containing or control medium are shown.

kocytes that remained attached to endothelial cells during the procedure. Pre-exposure to ADA increased the number of leukocytes attached to the endothelial monolayer by 33.0% at 48 h ($p < 0.05$) and 40.8% ($p < 0.05$) at 72 h (Fig. 6*B*). These findings are consistent with the increase of cell surface-detectable ICAM-1. The mean fluorescence intensity of the endothelial marker CD31 (platelet endothelial cell adhesion molecule 1 or PECAM-1), used to distinguish endothelial cells during the assay, was increased by 33.3% after 72 h of ADA treatment ($p < 0.0001$), suggesting that it may also be up-regulated under hypomethylating stress.

GPx-1 Expression Deregulation by Sec-tRNA Hypomethylation—During Sec incorporation, Sec-tRNA$^{[Ser]Sec}$ recognizes the stop codon, UGA, as a site for Sec insertion (8, 19, 43). As noted in the Introduction, mammalian tRNA$^{[Ser]Sec}$ is present in two main isoforms, which differ by a methyl group in the wobble uridine (U34) of the anticodon (Fig. 7*A*) (21). The mcm^{5}Um isoform of tRNA$^{[Ser]Sec}$ has been shown to be required for the expression of stress-related selenoproteins, which include GPx-1 (21, 23). To determine whether excess SAH altered the methylation state of the tRNA$^{[Ser]Sec}$, we treated cells with ADA and measured the levels of both isoforms, mcm^{5}U and mcm^{5}Um, following the specific labeling and chromatographic separation of [^{3}H]-Ser-tRNA$^{[Ser]Sec}$. Fig. 7*B* shows the chromatographic separation of the tRNA$^{[Ser]Sec}$ isoforms from control cells or cells under SAHH inhibition. Preparations from control cells (Fig. 7*B*, *left panel*) show two different peaks that represent the presence of the mcm^{5}U form (earlier-eluting peak) and the mcm^{5}Um form (later-eluting peak). Following ADA exposure, the tRNA$^{[Ser]Sec}$ mcm^{5}Um isoform is practically undetectable (Fig. 7*B*, *right panel*), suggesting that ADA treatment blocks the formation of the critical isoform of tRNA$^{[Ser]Sec}$ necessary for optimal Sec incorporation in GPx-1 and other selenoproteins. Interestingly, total tRNA$^{[Ser]Sec}$ levels were increased 1.7-fold with ADA exposure.

We next used [^{75}Se] labeling, followed by gel electrophoresis, to study the expression of key proteins in the selenoproteome (Fig. 7*C*). Overall, there are more than 25 selenoproteins that are encoded in 25 genes in humans (18, 44). To confirm the absence of changes in protein synthesis or other gel loading issues, β-actin immunoblotting was performed following radioautography of [^{75}Se]-labeled proteins. There were no differences detected in β-actin between control and treated samples. In contrast, examination of the [^{75}Se]-labeled proteins indicates alterations in selenoprotein expression in control cells compared with those in which SAH accumulation was induced. The molecular mass of selenoproteins, such as GPx-1, GPx-4, thioredoxin reductase (TrxR) 1, Sep15, and MsrB1, have been characterized previously in mammalian cells and tissues (23), and these can be identified by their relative migration in the gel imaged in Fig. 7*C*. Consistent with the results of Western blotting and activity assays, ADA and siSAHH decreased the [^{75}Se] labeling of GPx-1. The selenoproteins, GPx-4, Sep15, and/or MsrB1, were also suppressed by these treatments. Interestingly, the TrxR enzymes (TrxR1 and, to a lesser extent, TrxR2) showed increased expression. Western blot analysis was used to confirm the up-regulation of these TrxRs (Fig. 7*D*), illustrating the significant ($p < 0.05$) up-regulation of TrxR1 by 36.8% and TrxR2 by 23.1% following ADA treatment. TrxR1, but not TrxR2, mRNA was also significantly up-regulated (Fig. 7*E*), and cellular TrxR activity was also significantly increased by ADA exposure ($p < 0.05$) (Fig. 8*A*). These findings are consistent with previous studies that suggest that the expression of the TrxRs is less reliant on methylated tRNA$^{[Ser]Sec}$ than other selenoproteins, including GPx-1 (21, 23, 43).

Selenium Supplementation and Hypomethylation—To determine whether excess selenium would mitigate the effects of ADA on GPx-1 and TrxR expression, we added additional selenium to the culture medium, which had 37.5 nM selenium. Addition of up to 100 nM selenium for 4 days did not increase GPx-1 or TrxR1 in the absence of ADA (Fig. 8, *A* and *B*). Similarly, in the presence of ADA, exposure to additional selenium did not significantly alter the effects of ADA alone on GPx-1 or TrxR activity and expression, although, at 50 nM selenium plus ADA, there was a (non-significant) increase in GPx-1 protein. We next determined whether additional selenium altered ADA-induced adhesion molecule up-regulation (Fig. 8*C*). Western blot analysis showed that the ADA-induced up-regulation of ICAM-1 and VCAM-1 was unchanged by excess selenium.

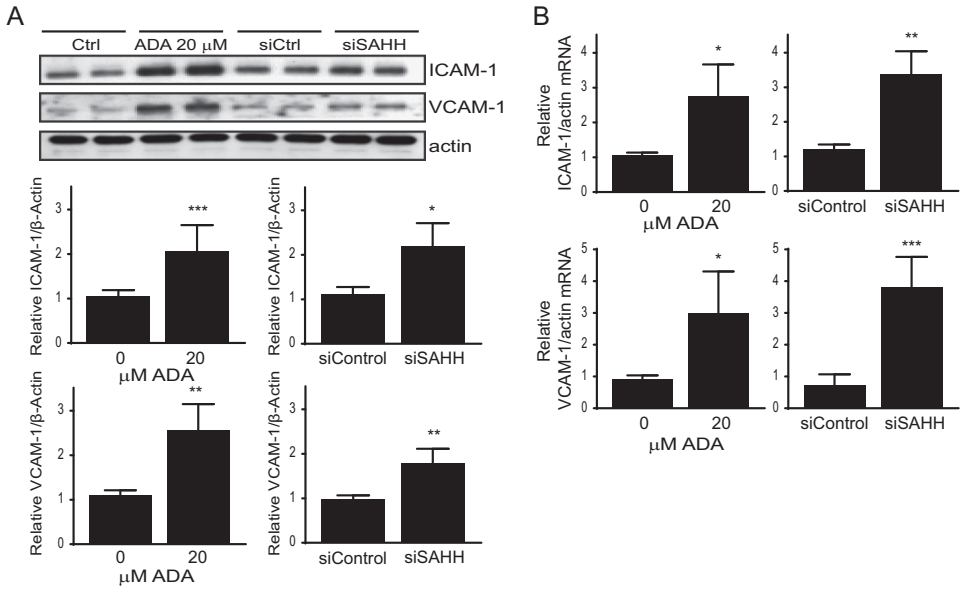

FIGURE 4. **Adhesion molecules expression is increased by pharmacological or siRNA-mediated suppression of SAHH.** *A*, the effect of 48 h of SAHH inhibition on the expression of ICAM-1 and VCAM-1 was evaluated by Western blotting. *Top panel*, a representative blot. *Bottom panel*, relative mean densitometry measurements, corrected for actin, for each protein and treatment condition. Mean densitometry measurements were compared by Student's *t* test ($n = 3$–5). *, $p < 0.05$; **, $p < 0.005$; ***, $p < 0.0005$. *Ctrl*, control. *B*, gene expression levels from the same experiments were measured by quantitative RT-PCR, using actin gene expression as a control. *, $p < 0.05$; **, $p < 0.005$; ***, $p < 0.0005$.

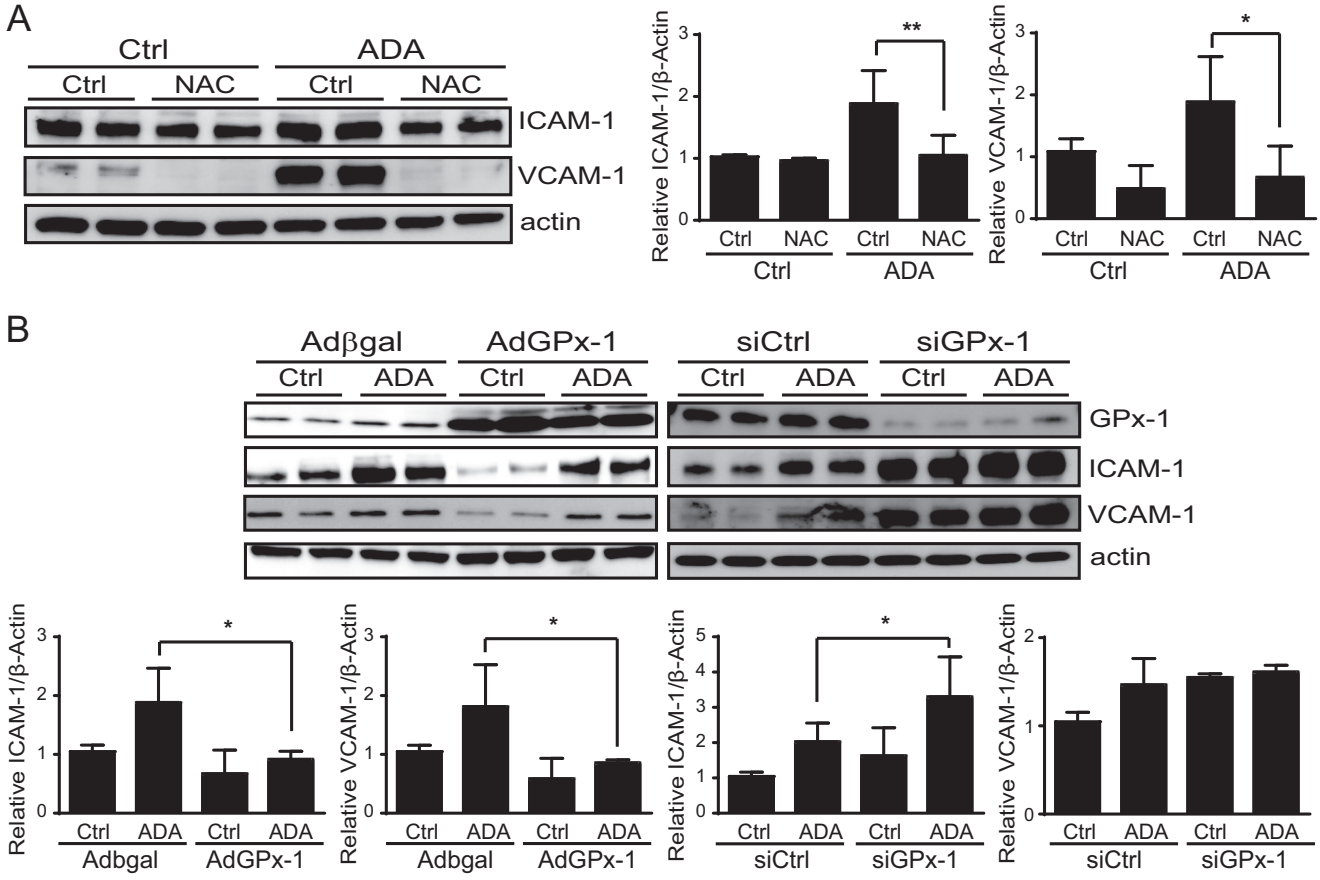

FIGURE 5. **Oxidative stress contributes to endothelial cell activation following SAHH inhibition.** *A*, control cells (*Ctrl*) or cells exposed to ADA were incubated in the presence or absence of the antioxidant *N*-acetylcysteine (*NAC*, 8 mM). Western blot analysis was performed to evaluate ICAM-1 and VCAM-1 protein expression. A representative blot is shown (*left panel*) as well as mean densitometry measurements, corrected for actin, for each protein and treatment condition (*right panel*). Densitometry results were analyzed by analysis of variance, followed by pairwise post hoc analysis. *, $p < 0.05$; **, $p < 0.005$. *B*, *left panel*, cells with overexpression of a control gene (β-Gal) or GPx-1 were incubated in the presence or absence of ADA. Western blotting was used to evaluate ICAM-1 and VCAM-1 expression. *Right panel*, ICAM-1 and VCAM-1 expression was evaluated in the presence or absence of ADA and GPx-1 knockdown. Mean densitometry measurements, normalized for actin, were analyzed as in *A*.

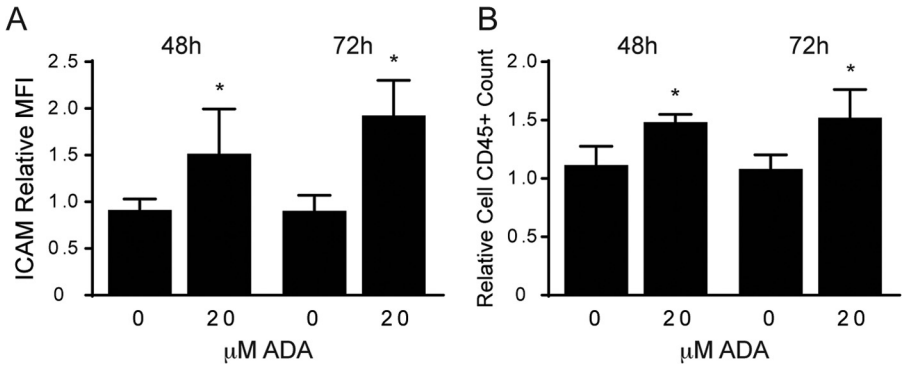

FIGURE 6. **Cell surface adhesion of leukocytes is enhanced by ADA exposure.** *A*, flow cytometry was used to detect cell surface expression of ICAM-1 tagged with a fluorescent antibody following exposure to ADA for 48 and 72 h ($n = 3$). Means were compared at each time point between ADA treatment and no treatment by Student's *t* test. *, $p < 0.05$. *MFI*, mean fluorescence intensity. *B*, following a static adhesion assay, leukocytes that remained attached to the endothelial monolayer were labeled with a fluorescence-conjugated antibody (CD45) and counted by FACS. Results are shown as means from three independent assays, normalized to the control and analyzed as in *A*. *, $p < 0.05$.

DISCUSSION

Methylation is essential for critical cell processes, including gene expression and protein function (45, 46). SAH, which is one of the most potent *in vivo* modulators of AdoMet-dependent methylation reactions, is an important regulator of cellular homeostasis. The AdoMet-to-SAH ratio is thought to regulate intracellular methylation reactions, with many methyltransferases showing diminished activity when this ratio decreases (4, 45). Altered methylation patterns have been related to cellular dysfunction and disease, including cancer and cardiovascular disease (45, 47, 48). RNA methylation can regulate the structure and function of various RNA species. tRNA is the most heavily modified RNA species, and modifications to nucleotides in the anticodon loop, especially at the wobble position (position 34), play an essential role in efficient mRNA decoding at the ribosome (49).

SAH, which accumulates in the setting of hyperhomocysteinemia, has gained attention as an intracellular metabolite that may be responsible for the deleterious actions on the vasculature attributed previously to excess Hcy (46). Our studies are focused on the effects of SAH as a hypomethylating agent that alters endothelial function. In particular, our results indicate that excess SAH decreases methylation of $tRNA^{[Ser]Sec}$ to alter the expression of the selenoproteins GPx-1 and TrxR. We show that the resulting decrease in the expression of the antioxidant selenoprotein GPx-1 leads to an increase in cellular H_2O_2 and a subsequent up-regulation of endothelial adhesion molecule expression. Furthermore, the increase in adhesion molecules is sufficient to have a functional effect on cellular adhesion, augmenting the binding of leukocytes. Recent studies have reported possible links between methylation impairment and vascular dysfunction (2, 50, 51). Here we demonstrate a specific mechanism by which hypomethylation stress can lead to inflammatory activation of endothelial cells.

In our study, we used two methodological approaches to promote SAH accumulation by targeting SAHH. First, we used the specific SAHH inhibitor ADA, which is known to cause SAH-induced hypomethylation stress (1, 2). Additionally, we used targeted siRNA-mediated knockdown of SAHH. Two additional genes that encode the SAHH-like proteins 1 and 2 have also been identified in mammalian systems (52, 53), although a clear functional role for these proteins has yet to be made. Nonetheless, in our targeted siRNA knockdown studies, we confirmed that siSAHH did not affect the levels of SAHH-like 1 and SAHH-like 2 mRNA. Overall, the effects of siSAHH paralleled those of SAHH inhibition, although the magnitude of the changes was lower with the siSAHH. This difference may be explained by the time course of their action because ADA has an almost immediate inhibitory action on SAHH activity, whereas the siRNA takes longer to achieve its maximal effect on SAHH expression. Moreover, siSAHH resulted in only a 67% reduction of SAHH activity compared with the complete suppression achieved with ADA. Nonetheless, targeted siRNA-mediated knockdown of SAHH had qualitatively similar effects on altering the AdoMet/SAH ratio as the pharmacological approach. An unanticipated result was the ADA-induced suppression of SAHH mRNA, although, under the time frame examined, this did not significantly alter SAHH protein expression. This may be the result of a feedback mechanism in which excess SAH suppresses SAHH expression.

Here we show that oxidative stress can be promoted by excess SAH. Our data are consistent with a role for hypomethylation in the suppression of GPx-1 expression (Fig. 2). Our previous studies indicated that excess exogenous Hcy, or conditions that promote Hcy production in cells, reduce GPx-1 expression by a mechanism that involved decreased selenium-dependent translation (7). GPx-1 is one of the major antioxidants that can modulate overall oxidative stress (8). Its role in vascular dysfunction has been studied widely as an important regulator of endothelial oxidative balance, and its deficiency contributes to atherosclerosis in susceptible mice and patients with coronary artery disease. Here we observed a decrease in GPx-1 activity and protein expression following pharmacological inhibition or knockdown of SAHH with no significant decrease in GPx-1 transcript levels. Taken together, these findings suggest that GPx-1 is modulated by hypomethylation post-transcriptionally. It has been suggested previously that the GPx-1 promoter is a target for epigenetic regulation by DNA methylation because exposure to the DNA methyltransferase inhibitor 5′-aza-2-deoxycytidine induced an up-regulation of GPx-1 in gastric carcinoma cells (54). In our study, however, hypomethylation stress did not increase GPx-1 expression.

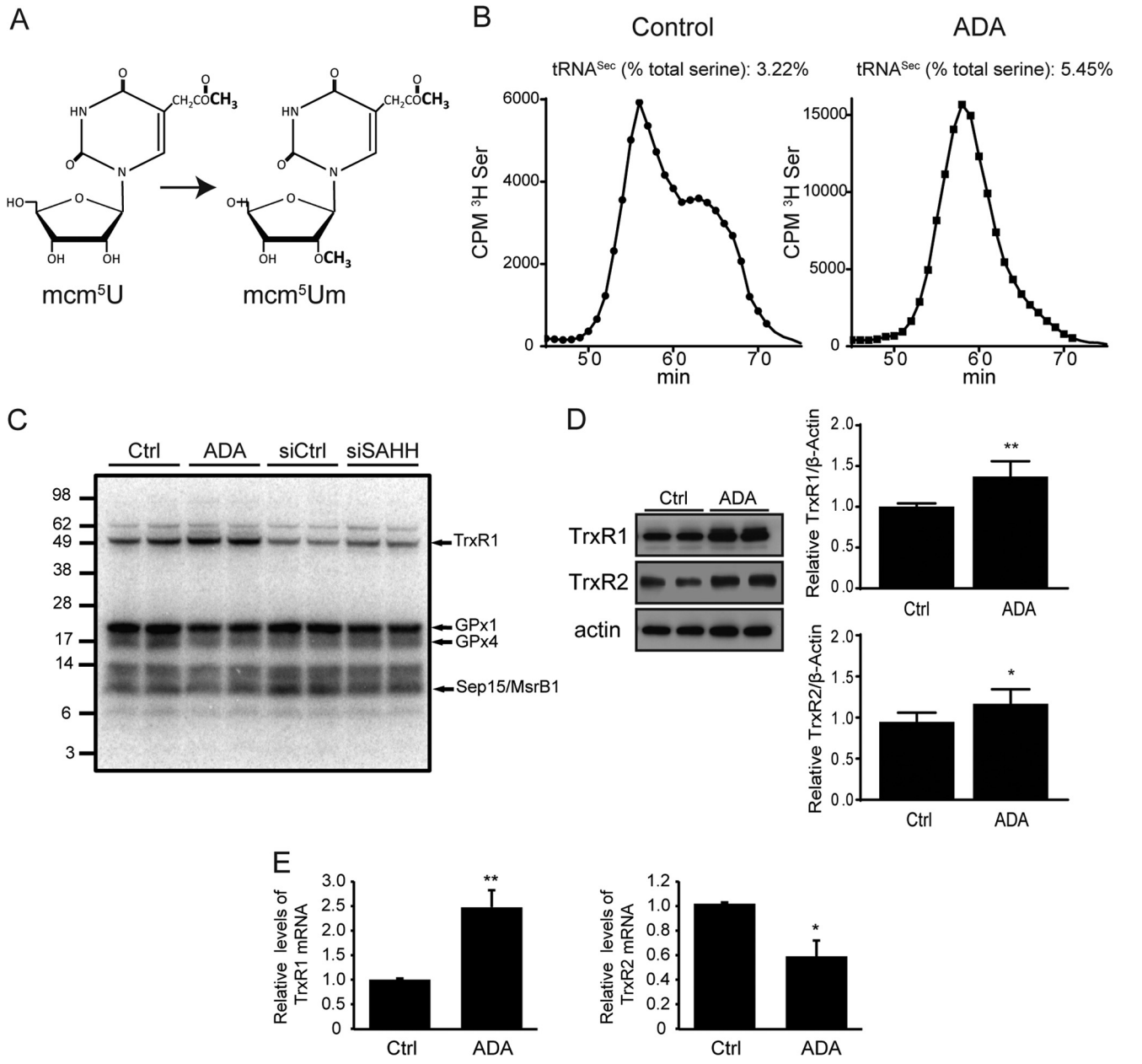

FIGURE 7. **tRNA$^{[Ser]Sec}$ hypomethylation and its effect on selenoproteome expression.** *A*, structures of the mcm^{5}U and mcm^{5}Um isoforms of the wobble uridine (Um34). *B*, following aminoacylation with [^{3}H]-serine, tRNA$^{[Ser]Sec}$ isoforms were separated by reverse phase chromatography. A normal profile is shown in the *left panel* (control cells), where mcm^{5}U elutes earlier than the mcm^{5}Um isoform. In the *right panel*, cells exposed to ADA are lacking the peak corresponding to the later-eluting mcm^{5}Um isoform. Note the differences in the *y* axis scales. *cpm*, counts per minute. *C*, duplicates of control cells (*Ctrl*) or cells exposed to ADA or siRNA treatment were labeled for 24 h with ^{75}Se. Proteins were extracted and separated by gel electrophoresis, and labeled selenoproteins were detected using a PhosphorImager. The protein marker sizes (in kilodalton) and selected selenoprotein bands are indicated on the *left* and *right* sides of the image, respectively. *D*, protein extracts were prepared from total cell lysates treated and untreated with ADA, and Western blot analyses were used to detect TrxR1 and TrxR2. A representative blot is shown. *Right panel*, relative mean densitometry measurements are shown, corrected for actin, for each protein and treatment condition. Mean densitometry measurements were compared by Student's *t* test ($n = 3$). *, $p < 0.05$; **, $p < 0.005$. *E*, TrxR1 and TrxR2 mRNA levels were measured in treated and untreated control samples by quantitative RT-PCR using actin as endogenous control.

Furthermore, in endothelial cells exposed to 5′-aza-2-deoxycytidine, we did not observe an up-regulation in GPx-1 expression (data not shown), suggesting that GPx-1 regulation by DNA methylation may be cell type-specific.

Our laboratory recently reported that GPx-1 deficiency is sufficient to augment the expression of ICAM-1 and VCAM-1 in human endothelial cells (14). Here we show that SAH accumulation also induces up-regulation of these adhesion molecules, possibly via the suppression of GPx-1 and the subsequent increase in cellular ROS (Fig. 9), which can activate signaling pathways that promote up-regulation of adhesion molecules (14). Furthermore, we confirmed a role for GPx-1 in the regulation of adhesion molecules by using gain and loss of function approaches. GPx-1 overexpression decreased ADA-induced adhesion molecule up-regulation, whereas its knockdown augmented the effects of hypomethylation on adhesion molecule up-regulation.

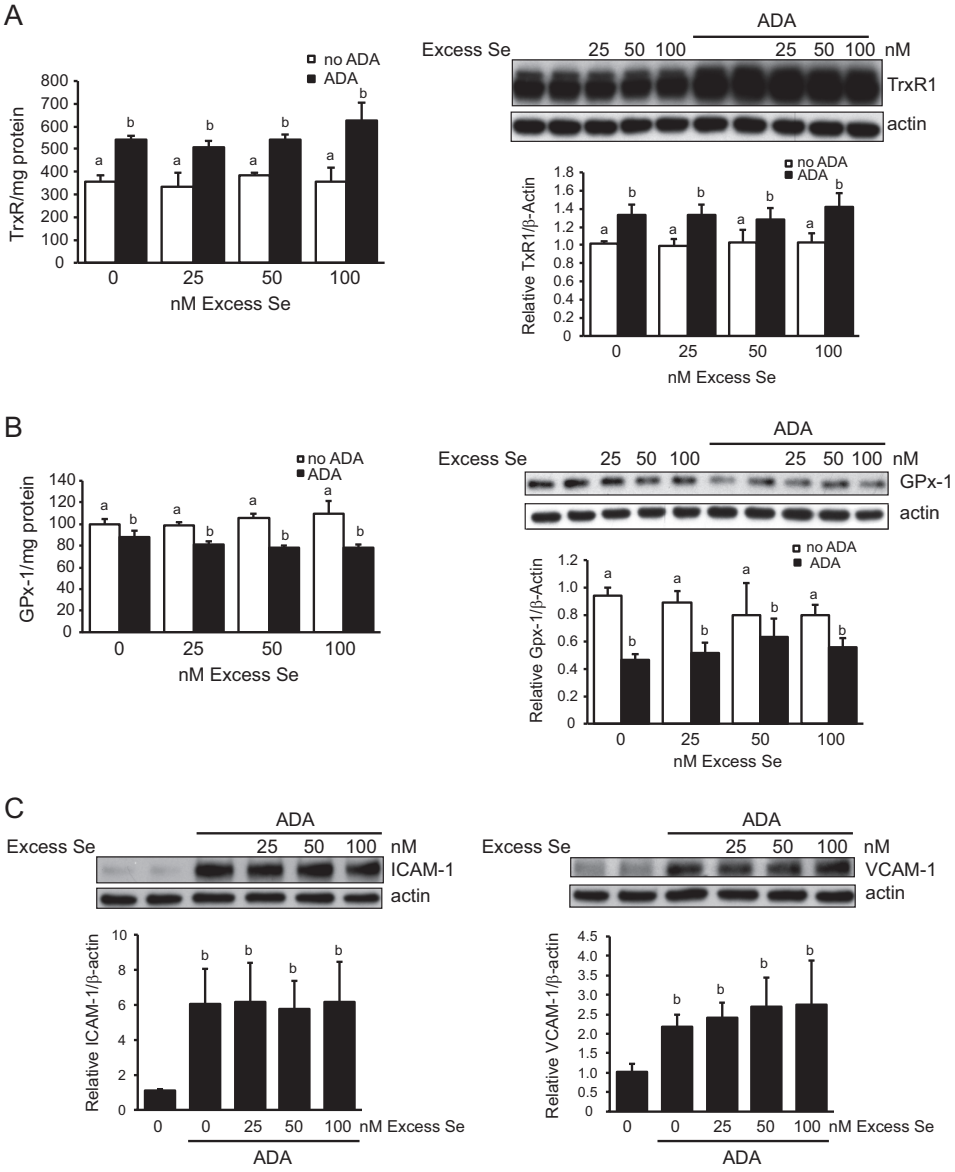

FIGURE 8. **The effects of excess selenium on TrxR1 and GPx-1 expression.** 48 h prior to ADA exposure sodium selenite was added to supplement medium that contained 37.5 nM selenium. Excess selenium concentrations were maintained throughout the subsequent 48-h ADA exposure. *A*, effect of excess selenium on TrxR enzyme activity and TrxR1 protein expression. Excess selenium had no effect on TrxR1 activity ($n = 3$) or expression ($n = 4$) in the absence of ADA. In the presence of ADA, the TrxR1 up-regulation of TrxR1 was not altered by excess selenium. *B*, effect of excess selenium on GPx-1 activity ($n = 4–6$) and GPx-1 protein expression ($n = 4$) in the presence and absence of ADA. Selenium did not significantly alter GPx-1 in the absence of ADA. In the presence of ADA, the suppression of GPx-1 was not decreased by excess selenium. *C*, effect of excess selenium on ICAM-1 and VCAM-1 protein. Excess selenium did not lessen ADA-induced up-regulation of the ICAM-1 or VCAM-1. For each graph, values that are not significantly different from no treatment or ADA are labeled *a* or *b*, respectively.

ICAM-1, VCAM-1, and PECAM-1 can mediate the adhesion of leukocytes to the endothelium and their transmigration (10, 11, 55). We demonstrated that hypomethylation stress in endothelial cells caused an increase in the cell surface expression of ICAM-1 and PECAM-1. Although the magnitude of the increase in cell surface ICAM-1 was less than the magnitude of the up-regulation in total ICAM-1 expression, increased cell surface expression of adhesion molecules following ADA exposure was sufficient to increase leukocyte binding. These findings suggest that the effects of hypomethylation may contribute to inflammatory proatherogenic changes in endothelial cells.

We further demonstrated a role for oxidants in the SAH-induced up-regulation of adhesion molecules because treatment with antioxidants attenuated the ADA-induced up-regulation of ICAM-1 and VCAM-1 (Fig. 5). Interestingly, other studies in cancer-associated endothelial cells suggest that the ICAM-1 gene promoter is a target for DNA methylation. Thus, its expression may also be regulated epigenetically (56). Nonetheless, a variety of antioxidant treatments lessened the expression of ICAM-1, as well as VCAM-1, in ADA-treated cells, suggesting that the SAH-induced reduction of GPx-1 and subsequent oxidant stress, rather than DNA hypomethylation, contribute to their up-regulation.

GPx-1 is a member of the selenoproteome, which comprises more than 25 proteins that contain selenium in the form of the Sec amino acid (18, 21, 44). More than 50% of the selenopro-

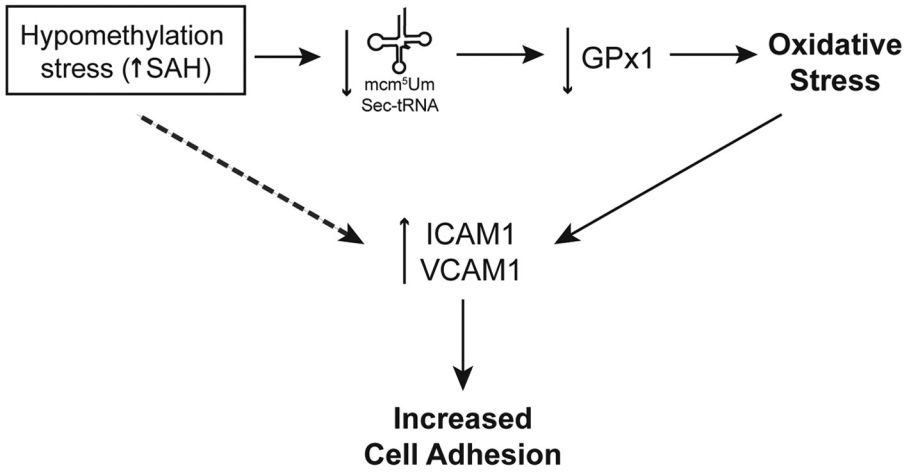

FIGURE 9. **The role of hypomethylation on endothelial dysfunction and activation.** Excess SAH induces hypomethylation stress capable of decreasing the available $tRNA^{[Ser]Sec}$ isoform mcm^5Um. Lack of this $tRNA^{[Ser]Sec}$ isoform decreases the expression of the antioxidant GPx-1 (as well as other selenoproteins). Loss of GPx-1 causes an increase in cellular oxidants, promoting oxidative stress. Oxidant stress contributes to increased expression of adhesion molecules that are responsible for an increased capacity to bind leukocytes, contributing to a proatherogenic environment. Other possible mechanisms (*dashed arrow*), such as DNA hypomethylation, may also be involved in the up-regulation of adhesion molecules such as ICAM-1 and VCAM-1.

teome is known to be involved in redox homeostasis, and selenium deficiency has been associated with oxidative stress and cancer (18). The unique translation mechanism exclusive to these proteins involves the recognition of the UGA codon, which, under most circumstances, signals translation termination, as a signal for Sec incorporation. Interestingly, Sec is synthesized directly on the tRNA that is initially charged with a Ser, which is subsequently converted enzymatically to Sec (20, 57). The two major $tRNA^{[Ser]Sec}$ isoforms, mcm^5U and mcm^5Um, which differ by a single methyl group, Um34, at position 34, modulate the expression of selenoproteins (21). Theoretically, SAH-induced hypomethylation of this tRNA will affect not only GPx-1 expression but also expression of other members of the selenoproteome. By using [^{75}Se] labeling, we found that many Sec-containing proteins were down-regulated following SAHH impairment. Previous studies have shown that some selenoproteins are less sensitive to the loss of the mcm^5Um isoform of $tRNA^{[Ser]Sec}$ than others. In particular, the mcm^5U isoform of $tRNA^{[Ser]Sec}$ supports the synthesis of a subclass of selenoproteins, designated as housekeeping selenoproteins (TrxR1 and TrxR2), whereas the methylated mcm^5Um form supports the expression of the stress-related subclass of selenoproteins (GPx-1, GPx-3, GPx-4, SelR, SelT, and SelW) (21). Accordingly, among the proteins that can be identified following selenium labeling, we found that hypomethylation results in an increase in TrxR1 expression, whereas GPx-1 and GPx-4 are diminished. One limitation of our study is that we have not confirmed the suppressive effects of ADA on selenoproteins other than GPx-1. Our results, however, clearly demonstrate a reciprocal regulation of TrxR1 and GPx-1, with a Pearson's correlation coefficient of -0.647, $p = 0.0006$, between TrxR and GPx-1 enzyme activities. Interestingly, protein expression of the related TrxR1 and TrxR2 were both increased by ADA, although the mechanisms may be different. Only the TrxR1 mRNA was increased with exposure to ADA. It is well known that TxR1 is a target for transcriptional regulation by the stress-activated nuclear factor Nrf2 (58–60). Thus, oxidant stress caused by GPx-1 suppression may contribute to TxR1 up-regulation, although other factors may also play a role in augmenting TxR1 expression. The reciprocal regulation of TrxR1 and GPx-1 has been reported previously in a variety of cancer cells (61), and these antioxidant enzymes may have complementary roles in regulating cellular redox. Thus, similar to loss of GPx-1, knockdown of TrxR1 may increase H_2O_2 in endothelial cells, although, of the TrxR enzymes, the TrxR2 appears to have a greater role in modulating intracellular H_2O_2 (62). In this study, however, modest up-regulation of TrxR enzymes was not sufficient to compensate for suppression of GPx-1 because H_2O_2 accumulated in ADA-treated endothelial cells.

In our cell culture system, HUVECs were cultured with medium containing 30 nM selenious acid plus 7.5 nM selenium from serum. The addition of excess selenium up to 100 nM had little effect on the expression of GPx-1 or TrxR, as monitored by Western blot analyses and enzyme activity assays (Fig. 8). The lack of an effect of additional selenium in our cell system is consistent with previous studies reporting maximal expression of TrxR and GPx-1 when endothelial cells were cultured with 40 nM selenium (63).

To date, the methyltransferase responsible for the methylation of mcm^5U $tRNA^{[Ser]Sec}$ has not been identified, but our studies suggest that it may be particularly sensitive to SAH accumulation because its product is virtually undetectable after ADA treatment (Fig. 7*B*). Recent studies have identified a methyltransferase, ALKBH8, that, when complexed with TRM112, catalyzes the methyl esterification of cm^5U to mcm^5U (64, 65). Absence of ALKBH8 also inhibited the decoding of the UGA stop codon to Sec, causing reduced levels of GPx-1 in the liver of ALKBH8-deficient mice (64).

Interestingly, besides the lack of the methylated form of $tRNA^{[Ser]Sec}$, cells under SAH accumulation appeared to respond to the absence of this isoform by inducing $tRNA^{[Ser]Sec}$ production. ADA treatment caused an approximately 1.7-fold increase in the overall levels of $tRNA^{[Ser]Sec}$. The mechanism that regulates this feedback response is not clear and needs further investigation.

Our work elucidates a new mechanism by which hypomethylation can modulate selenoprotein expression. Because excess SAH can be found under conditions of elevated Hcy and because it inhibits methylation reactions, we propose that SAH accumulation may explain the effects of Hcy on GPx-1 suppression. Fig. 9 summarizes the mechanism by which a hypomethylating environment can contribute to endothelial dysfunction and activation. Thus, an accumulation of SAH inhibits the methylation of the $tRNA^{[Ser]Sec}$ necessary for efficient translation of GPx-1 and other selenoproteins. The impairment of this important antioxidant can lead to oxidant stress and endothelial activation, contributing to the up-regulation of ICAM-1 and VCAM-1 adhesion molecules, which may augment leukocyte binding to contribute to an atherogenic phenotype.

Acknowledgments—We thank Derrick Kao (Brigham and Women's Hospital, Harvard Medical School) for technical assistance and Desirée Smith (VU University Medical Center, The Netherlands) for help with AdoMet and SAH quantification and analysis. We also thank Stephanie Tribuna for expert technical assistance.

REFERENCES

1. Barroso, M., Rocha, M. S., Esse, R., Gonçalves, I., Jr., Gomes, A. Q., Teerlink, T., Jakobs, C., Blom, H. J., Loscalzo, J., Rivera, I., de Almeida, I. T., and Castro, R. (2012) Cellular hypomethylation is associated with impaired nitric oxide production by cultured human endothelial cells. *Amino Acids* **42,** 1903–1911
2. Esse, R., Rocha, M. S., Barroso, M., Florindo, C., Teerlink, T., Kok, R. M., Smulders, Y. M., Rivera, I., Leandro, P., Koolwijk, P., Castro, R., Blom, H. J., and de Almeida, I. T. (2013) Protein arginine methylation is more prone to inhibition by *S*-adenosylhomocysteine than DNA methylation in vascular endothelial cells. *PLoS ONE* **8,** e55483
3. Castro, R., Rivera, I., Struys, E. A., Jansen, E. E., Ravasco, P., Camilo, M. E., Blom, H. J., Jakobs, C., and Tavares de Almeida, I. (2003) Increased homocysteine and *S*-adenosylhomocysteine concentrations and DNA hypomethylation in vascular disease. *Clin. Chem.* **49,** 1292–1296
4. Caudill, M. A., Wang, J. C., Melnyk, S., Pogribny, I. P., Jernigan, S., Collins, M. D., Santos-Guzman, J., Swendseid, M. E., Cogger, E. A., and James, S. J. (2001) Intracellular *S*-adenosylhomocysteine concentrations predict global DNA hypomethylation in tissues of methyl-deficient cystathionine β-synthase heterozygous mice. *J. Nutr.* **131,** 2811–2818
5. Esse, R., Florindo, C., Imbard, A., Rocha, M. S., de Vriese, A. S., Smulders, Y. M., Teerlink, T., Tavares de Almeida, I., Castro, R., and Blom, H. J. (2013) Global protein and histone arginine methylation are affected in a tissue-specific manner in a rat model of diet-induced hyperhomocysteinemia. *Biochim. Biophys. Acta* **1832,** 1708–1714
6. Esse, R., Imbard, A., Florindo, C., Gupta, S., Quinlivan, E. P., Davids, M., Teerlink, T., Tavares de Almeida, I., Kruger, W. D., Blom, H. J., and Castro, R. (2014) Protein arginine hypomethylation in a mouse model of cystathionine β-synthase deficiency. *FASEB J.* 10.1096/fj.13-246579
7. Handy, D. E., Zhang, Y., and Loscalzo, J. (2005) Homocysteine down-regulates cellular glutathione peroxidase (GPx1) by decreasing translation. *J. Biol. Chem.* **280,** 15518–15525
8. Lubos, E., Loscalzo, J., and Handy, D. E. (2011) Glutathione peroxidase-1 in health and disease: from molecular mechanisms to therapeutic opportunities. *Antioxid. Redox Signal.* **15,** 1957–1997
9. Pastori, D., Carnevale, R., and Pignatelli, P. (2014) Is there a clinical role for oxidative stress biomarkers in atherosclerotic diseases? *Intern. Emerg. Med.* **9,** 123–131
10. Cook-Mills, J. M., Marchese, M. E., and Abdala-Valencia, H. (2011) Vascular cell adhesion molecule-1 expression and signaling during disease: regulation by reactive oxygen species and antioxidants. *Antioxid. Redox Signal.* **15,** 1607–1638
11. Förstermann, U. (2008) Oxidative stress in vascular disease: causes, defense mechanisms and potential therapies. *Nat. Clin. Pract. Cardiovasc. Med.* **5,** 338–349
12. Hulsmans, M., Van Dooren, E., and Holvoet, P. (2012) Mitochondrial reactive oxygen species and risk of atherosclerosis. *Curr. Atheroscler. Rep.* **14,** 264–276
13. Weber, C., and Noels, H. (2011) Atherosclerosis: current pathogenesis and therapeutic options. *Nat. Med.* **17,** 1410–1422
14. Lubos, E., Kelly, N. J., Oldebeken, S. R., Leopold, J. A., Zhang, Y. Y., Loscalzo, J., and Handy, D. E. (2011) Glutathione peroxidase-1 deficiency augments proinflammatory cytokine-induced redox signaling and human endothelial cell activation. *J. Biol. Chem.* **286,** 35407–35417
15. Lubos, E., Mahoney, C. E., Leopold, J. A., Zhang, Y. Y., Loscalzo, J., and Handy, D. E. (2010) Glutathione peroxidase-1 modulates lipopolysaccharide-induced adhesion molecule expression in endothelial cells by altering CD14 expression. *FASEB J.* **24,** 2525–2532
16. Lewis, P., Stefanovic, N., Pete, J., Calkin, A. C., Giunti, S., Thallas-Bonke, V., Jandeleit-Dahm, K. A., Allen, T. J., Kola, I., Cooper, M. E., and de Haan, J. B. (2007) Lack of the antioxidant enzyme glutathione peroxidase-1 accelerates atherosclerosis in diabetic apolipoprotein E-deficient mice. *Circulation* **115,** 2178–2187
17. Blankenberg, S., Rupprecht, H. J., Bickel, C., Torzewski, M., Hafner, G., Tiret, L., Smieja, M., Cambien, F., Meyer, J., Lackner, K. J., and AtheroGene, I. (2003) Glutathione peroxidase 1 activity and cardiovascular events in patients with coronary artery disease. *N. Engl. J. Med.* **349,** 1605–1613
18. Papp, L. V., Lu, J., Holmgren, A., and Khanna, K. K. (2007) From selenium to selenoproteins: synthesis, identity, and their role in human health. *Antioxid. Redox Signal.* **9,** 775–806
19. Donovan, J., and Copeland, P. R. (2010) Threading the needle: getting selenocysteine into proteins. *Antioxid. Redox Signal.* **12,** 881–892
20. Xu, X. T., A. A., Carlson, B. A., Yoo, M., Gladyshev, V. N., and Hatfield, D. L. (2012) in *Selenium: Its Molecular Biology and Role in Human Health* (Hatfield, D. L., Berry, M. J., and Gladyshev, V. N. eds) pp. 23–32 Springer, New York
21. Hatfield, D. L., Carlson, B. A., Xu, X. M., Mix, H., and Gladyshev, V. N. (2006) Selenocysteine incorporation machinery and the role of selenoproteins in development and health. *Prog. Nucleic Acid Res. Mol. Biol.* **81,** 97–142
22. Kim, L. K., Matsufuji, T., Matsufuji, S., Carlson, B. A., Kim, S. S., Hatfield, D. L., and Lee, B. J. (2000) Methylation of the ribosyl moiety at position 34 of selenocysteine tRNA[Ser]Sec is governed by both primary and tertiary structure. *RNA* **6,** 1306–1315
23. Carlson, B. A., Xu, X. M., Gladyshev, V. N., and Hatfield, D. L. (2005) Selective rescue of selenoprotein expression in mice lacking a highly specialized methyl group in selenocysteine tRNA. *J. Biol. Chem.* **280,** 5542–5548
24. Struys, E. A., Jansen, E. E., de Meer, K., and Jakobs, C. (2000) Determination of *S*-adenosylmethionine and *S*-adenosylhomocysteine in plasma and cerebrospinal fluid by stable-isotope dilution tandem mass spectrometry. *Clin. Chem.* **46,** 1650–1656
25. Kloor, D., Hermes, M., Fink, K., Schmid, H., Klingel, K., Mack, A., Grenz, A., and Osswald, H. (2007) Expression and localization of *S*-adenosylhomocysteine-hydrolase in the rat kidney following carbon monoxide induced hypoxia. *Cell. Physiol. Biochem.* **19,** 57–66
26. Kloor, D., Stumvoll, W., Schmid, H., Kömpf, J., Mack, A., and Osswald, H. (2000) Localization of *S*-adenosylhomocysteine hydrolase in the rat kidney. *J. Histochem. Cytochem.* **48,** 211–218
27. Turanov, A. A., Su, D., and Gladyshev, V. N. (2006) Characterization of alternative cytosolic forms and cellular targets of mouse mitochondrial thioredoxin reductase. *J. Biol. Chem.* **281,** 22953–22963
28. Arnér, E. S., Zhong, L., and Holmgren, A. (1999) Preparation and assay of mammalian thioredoxin and thioredoxin reductase. *Methods Enzymol.* **300,** 226–239
29. Smith, A. D., and Levander, O. A. (2002) High-throughput 96-well microplate assays for determining specific activities of glutathione peroxidase and thioredoxin reductase. *Methods Enzymol.* **347,** 113–121
30. Handy, D. E., Lubos, E., Yang, Y., Galbraith, J. D., Kelly, N., Zhang, Y. Y., Leopold, J. A., and Loscalzo, J. (2009) Glutathione peroxidase-1 regulates

mitochondrial function to modulate redox-dependent cellular responses. *J. Biol. Chem.* **284,** 11913–11921
31. Belousov, V. V., Fradkov, A. F., Lukyanov, K. A., Staroverov, D. B., Shakhbazov, K. S., Terskikh, A. V., and Lukyanov, S. (2006) Genetically encoded fluorescent indicator for intracellular hydrogen peroxide. *Nat. Methods* **3,** 281–286
32. Sartoretto, J. L., Kalwa, H., Pluth, M. D., Lippard, S. J., and Michel, T. (2011) Hydrogen peroxide differentially modulates cardiac myocyte nitric oxide synthesis. *Proc. Natl. Acad. Sci.* **108,** 15792–15797
33. Kalwa, H., Sartoretto, J. L., Sartoretto, S. M., and Michel, T. (2012) Angiotensin-II and MARCKS: a hydrogen peroxide- and RAC1-dependent signaling pathway in vascular endothelium. *J. Biol. Chem.* **287,** 29147–29158
34. Yoo, M. H., Xu, X. M., Turanov, A. A., Carlson, B. A., Gladyshev, V. N., and Hatfield, D. L. (2007) A new strategy for assessing selenoprotein function: siRNA knockdown/knock-in targeting the 3′-UTR. *RNA* **13,** 921–929
35. Moustafa, M. E., Carlson, B. A., El-Saadani, M. A., Kryukov, G. V., Sun, Q. A., Harney, J. W., Hill, K. E., Combs, G. F., Feigenbaum, L., Mansur, D. B., Burk, R. F., Berry, M. J., Diamond, A. M., Lee, B. J., Gladyshev, V. N., and Hatfield, D. L. (2001) Selective inhibition of selenocysteine tRNA maturation and selenoprotein synthesis in transgenic mice expressing isopentenyladenosine-deficient selenocysteine tRNA. *Mol. Cell. Biol.* **21,** 3840–3852
36. Kumaraswamy, E., Carlson, B. A., Morgan, F., Miyoshi, K., Robinson, G. W., Su, D., Wang, S., Southon, E., Tessarollo, L., Lee, B. J., Gladyshev, V. N., Hennighausen, L., and Hatfield, D. L. (2003) Selective removal of the selenocysteine tRNA [Ser]Sec gene (Trsp) in mouse mammary epithelium. *Mol. Cell. Biol.* **23,** 1477–1488
37. Déry, U., Coulombe, Y., Rodrigue, A., Stasiak, A., Richard, S., and Masson, J. Y. (2008) A glycine-arginine domain in control of the human MRE11 DNA repair protein. *Mol. Cell. Biol.* **28,** 3058–3069
38. Schnabel, R., Lackner, K. J., Rupprecht, H. J., Espinola-Klein, C., Torzewski, M., Lubos, E., Bickel, C., Cambien, F., Tiret, L., Münzel, T., and Blankenberg, S. (2005) Glutathione peroxidase-1 and homocysteine for cardiovascular risk prediction: results from the AtheroGene study. *J. Am. Coll. Cardiol.* **45,** 1631–1637
39. Weiss, N., Zhang, Y. Y., Heydrick, S., Bierl, C., and Loscalzo, J. (2001) Overexpression of cellular glutathione peroxidase rescues homocyst(e)ine-induced endothelial dysfunction. *Proc. Natl. Acad. Sci.* **98,** 12503–12508
40. Le, N. T., Corsetti, J. P., Dehoff-Sparks, J. L., Sparks, C. E., Fujiwara, K., and Abe, J. (2012) Reactive oxygen species, SUMOylation, and endothelial inflammation. *Int. J. Inflam.* **2012,** 678190
41. Rahman, A., and Fazal, F. (2009) Hug tightly and say goodbye: role of endothelial ICAM-1 in leukocyte transmigration. *Antioxid. Redox Signal.* **11,** 823–839
42. Roebuck, K. A., and Finnegan, A. (1999) Regulation of intercellular adhesion molecule-1 (CD54) gene expression. *J. Leukoc. Biol.* **66,** 876–888
43. Howard, M. T., Carlson, B. A., Anderson, C. B., and Hatfield, D. L. (2013) Translational redefinition of UGA codons is regulated by selenium availability. *J. Biol. Chem.* **288,** 19401–19413
44. Kryukov, G. V., Castellano, S., Novoselov, S. V., Lobanov, A. V., Zehtab, O., Guigó, R., and Gladyshev, V. N. (2003) Characterization of mammalian selenoproteomes. *Science* **300,** 1439–1443
45. King, W. D., Ho, V., Dodds, L., Perkins, S. L., Casson, R. I., and Massey, T. E. (2012) Relationships among biomarkers of one-carbon metabolism. *Mol. Biol. Rep.* **39,** 7805–7812
46. Xiao, Y., Zhang, Y., Wang, M., Li, X., Su, D., Qiu, J., Li, D., Yang, Y., Xia, M., and Ling, W. (2013) Plasma *S*-adenosylhomocysteine is associated with the risk of cardiovascular events in patients undergoing coronary angiography: a cohort study. *Am. J. Clin. Nutr.* **98,** 1162–1169
47. Shen, H., and Laird, P. W. (2013) Interplay between the cancer genome and epigenome. *Cell* **153,** 38–55
48. Kim, G. H., Ryan, J. J., and Archer, S. L. (2013) The role of redox signaling in epigenetics and cardiovascular disease. *Antioxid. Redox Signal.* **18,** 1920–1936
49. Motorin, Y., and Helm, M. (2011) RNA nucleotide methylation. *Wiley Interdiscip. Rev. RNA* **2,** 611–631
50. Yan, M. S., Matouk, C. C., and Marsden, P. A. (2010) Epigenetics of the vascular endothelium. *J. Appl. Physiol.* **109,** 916–926
51. Polotskaia, A., Wang, M., Patschan, S., Addabbo, F., Chen, J., and Goligorsky, M. S. (2007) Regulation of arginine methylation in endothelial cells: role in premature senescence and apoptosis. *Cell Cycle* **6,** 2524–2530
52. Jeong, W., Kim, J., Ahn, S. E., Lee, S. I., Bazer, F. W., Han, J. Y., and Song, G. (2012) AHCYL1 is mediated by estrogen-induced ERK1/2 MAPK cell signaling and microRNA regulation to effect functional aspects of the avian oviduct. *PLoS ONE* **7,** e49204
53. Frazier-Wood, A. C., Aslibekyan, S., Borecki, I. B., Hopkins, P. N., Lai, C. Q., Ordovas, J. M., Straka, R. J., Tiwari, H. K., and Arnett, D. K. (2012) Genome-wide association study indicates variants associated with insulin signaling and inflammation mediate lipoprotein responses to fenofibrate. *Pharmacogen. Genomics* **22,** 750–757
54. Jee, C. D., Kim, M. A., Jung, E. J., Kim, J., and Kim, W. H. (2009) Identification of genes epigenetically silenced by CpG methylation in human gastric carcinoma. *Eur. J. Cancer* **45,** 1282–1293
55. Privratsky, J. R., Newman, D. K., and Newman, P. J. (2010) PECAM-1: conflicts of interest in inflammation. *Life Sci.* **87,** 69–82
56. Hellebrekers, D. M., Castermans, K., Viré, E., Dings, R. P., Hoebers, N. T., Mayo, K. H., Oude Egbrink, M. G., Molema, G., Fuks, F., van Engeland, M., and Griffioen, A. W. (2006) Epigenetic regulation of tumor endothelial cell anergy: silencing of intercellular adhesion molecule-1 by histone modifications. *Cancer Res.* **66,** 10770–10777
57. Xu, X. M., Carlson, B. A., Mix, H., Zhang, Y., Saira, K., Glass, R. S., Berry, M. J., Gladyshev, V. N., and Hatfield, D. L. (2007) Biosynthesis of selenocysteine on its tRNA in eukaryotes. *PLoS Biol.* **5,** e4
58. Sakurai, A., Nishimoto, M., Himeno, S., Imura, N., Tsujimoto, M., Kunimoto, M., and Hara, S. (2005) Transcriptional regulation of thioredoxin reductase 1 expression by cadmium in vascular endothelial cells: role of NF-E2-related factor-2. *J. Cell. Physiol.* **203,** 529–537
59. Fourquet, S., Guerois, R., Biard, D., and Toledano, M. B. (2010) Activation of NRF2 by nitrosative agents and H2O2 involves KEAP1 disulfide formation. *J. Biol. Chem.* **285,** 8463–8471
60. Brigelius-Flohe, R., Muller, M., Lippmann, D., and Kipp, A. P. The yin and yang of nrf2-regulated selenoproteins in carcinogenesis. (2012) *Int. J. Cell Biol.* **2012,** 486147
61. Gladyshev, V. N., Factor, V. M., Housseau, F., and Hatfield, D. L. (1998) Contrasting patterns of regulation of the antioxidant selenoproteins, thioredoxin reductase, and glutathione peroxidase, in cancer cells. *Biochem. Biophys. Res. Commun.* **251,** 488–493
62. Sugiyama, T., and Michel, T. (2010) Thiol-metabolizing proteins and endothelial redox state: differential modulation of eNOS and biopterin pathways. *Am. J. Physiol. Heart Circ. Physiol.* **298,** H194–201
63. Miller, S., Walker, S. W., Arthur, J. R., Nicol, F., Pickard, K., Lewin, M. H., Howie, A. F., and Beckett, G. J. (2001) Selenite protects human endothelial cells from oxidative damage and induces thioredoxin reductase. *Clin. Sci.* **100,** 543–550
64. Songe-Møller, L., van den Born, E., Leihne, V., Vågbø, C. B., Kristoffersen, T., Krokan, H. E., Kirpekar, F., Falnes, P. Ø., and Klungland, A. (2010) Mammalian ALKBH8 possesses tRNA methyltransferase activity required for the biogenesis of multiple wobble uridine modifications implicated in translational decoding. *Mol. Cell. Biol.* **30,** 1814–1827
65. Fu, D., Brophy, J. A., Chan, C. T., Atmore, K. A., Begley, U., Paules, R. S., Dedon, P. C., Begley, T. J., and Samson, L. D. (2010) Human AlkB homolog ABH8 is a tRNA methyltransferase required for wobble uridine modification and DNA damage survival. *Mol. Cell. Biol.* **30,** 2449–2459